

What Can We Learn from the Travelers Data in Detecting Disease Outbreaks– A Case Study of the COVID-19 Epidemic

Le Bao, Ying Zhang, Xiaoyue Niu

*Department of Statistics, Penn State University
University Park, PA 16802*

Abstract

Background: Travel is a potent force in the emergence of disease. We discussed how the traveler case reports could aid in a timely detection of a disease outbreak.

Methods: Using the traveler data, we estimated a few indicators of the epidemic that affected decision making and policy, including the exponential growth rate, the doubling time, and the probability of severe cases exceeding the hospital capacity, in the initial phase of the COVID-19 epidemic in multiple countries. We imputed the arrival dates when they were missing. We compared the estimates from the traveler data to the ones from domestic data. We quantitatively evaluated the influence of each case report and knowing the arrival date on the estimation. We developed a simple disease detection criterion that could help make future decisions.

Findings: Using only the travel report data, we estimated the travel origin's daily exponential growth rate in a moving window fashion that mimic the reality, and examined the date from which the growth rate was consistently above 0.1 (equivalent to doubling time < 7 days). We found those dates were very close to the dates that critical decisions were made such as city lock-downs and national emergency announcement. In addition, our estimated probability of severe cases exceeding the hospital capacity hit above 0.9 on the day Wuhan announced lock-down. Using only the traveler data, if the assumed epidemic start date was relatively accurate and the traveler sample was representative of the general population, the growth rate estimated from the traveler data was consistent with the domestic data. We also discussed situations that the traveler data could lead to biased estimates. From the

data influence study, we found more recent travel cases had a larger influence on each day’s estimate, and the influence of each case report got smaller as more cases became available. We provided the minimum number of exported cases needed to determine whether the local epidemic growth rate was above a certain level, and developed a user-friendly Shiny App to accommodate various scenarios.

Interpretation: The traveler data are useful information that help the early detection of a disease outbreak in the travel origin. The traveler data also have limitations that would need further information to refine. We advocate that countries should work in a collaborative way to share the traveler information about the travel dates and more detailed travel history at sub-national level, in a timely manner.

Funding: NIH/NIAID 5R01AI136664

Keywords: Disease Outbreaks, Traveler Case Report, Value of Information

1. Introduction

Since 2014, there have been five “public health emergency of international concern” (PHEIC) declarations including the most recent outbreak of COVID-19 [1]. Major challenges in early warning and rapid response to an emerging disease outbreak include the lack of epidemiological and laboratory techniques where disease started, and the fear of the negative impact that reporting the outbreak would have on trade and tourism [2, 3]. At the same time, travel is a potent force in the emergence of disease [4]. Travelers play a key role in a disease spreading out from local to global.

We believe that the case reports among travelers are informative data source for detecting the disease outbreaks. The WHO International Health Regulations (IHR) provided the instructions for nations to report diseases found in incoming travelers, and the regulations were revised to accommodate warnings of unknown infectious diseases [3]. [5] estimated the outbreak size of 2019-nCoV in Wuhan from the number of confirmed cases that have been exported to cities outside mainland China shortly after the lockdown in Wuhan. Other early studies that estimated the outbreak size in Wuhan using the cases exported include [6, 7].

In this article, we used the travelers data to estimate two important quantitative measures, the exponential growth rate (equivalent to doubling time) and the probability of severe cases exceeding hospital capacity, to detect the

disease outbreak in five travel origins (origins), Wuhan (China), Egypt, Iran, Italy, and United States. We investigated the contributions and limitations of traveler data on understanding the COVID-19 epidemic at its beginning stage. Our main contributions to the literature include: 1. Instead of using accumulated traveler cases up to a certain time point to get one estimate, we provided daily estimates so that we could see how the estimates of the key measures were evolving in the early stage. 2. A lot of the traveler case reports only provided the dates when travelers tested positive, without their actual arrival dates. We demonstrated that the arrival date was important in estimating those key measures and provided a probability model to impute the arrival date. 3. We used a statistically rigorous way to evaluate the influence of each case report and knowing the arrival dates on estimating the exponential growth rate. 4. We used the travel origin’s domestic data to benchmark the estimates from the travel case report and pointed out that there was a potential sampling bias in the travelers population so that the prevalence estimated from the traveler data might be different from the domestic estimate. We made the first attempt to adjust the bias but also acknowledge that we would need further information about the difference between travelers and the general population to fully address this issue. 5. We provided a simple criterion to determine the severity of the local epidemic based on the cumulative number of exported cases, and developed an easy-to-use app for practical usage. Finally, we discussed how to enhance global infectious disease surveillance by utilizing traveler case reports in a collaborative way.

2. Methods

2.1. Data Sources

We chose five places (four countries and one city) whose COVID-19 outbreaks were detected relatively early in their region as illustrative examples of travel origins. They were Wuhan (China), Italy, Iran, Egypt and United States. For each origin, we investigated the exported cases in the early stage of the country’s epidemic. We picked the start date as the date when the country announced its first confirmed case. We picked the end date as the date the country announced national emergency or implemented lock-down order. Table 1 summarizes the start date, the end date, the total number of exported traveler case reports and the total number of exported destinations within the study period. Without the daily travel volume, we assumed that

the travel volume to each destination was constant over this short period of time. The reasons for using those dates and the associated travel volume data are provided in Appendix A.1.

Table 1: The start date of the local epidemic, the end date of study period, the total number of exported traveler case reports within the study period, and the total number of exported destinations within the study period.

	start date of the local epidemic	end date of the study period	number of exported cases	number of destinations
Wuhan	Dec 1, 2019	Jan 23, 2020	11 cases	7 destinations
U.S.	Jan 20, 2020	Mar 13, 2020	25 cases	5 destinations
Italy	Jan 31, 2020	Feb 28, 2020	57 cases	19 destinations
Iran	Feb 19, 2020	Feb 27, 2020	90 cases	12 destinations
Egypt	Feb 14, 2020	Mar 6, 2020	9 cases	4 destinations

We obtained the traveler case reports within the period specified above from [8] with re-verification of their travel histories using government and media reports. Our analysis focused on the infections that likely occurred in the origin rather than transmitted during the trip. Therefore, we counted multiple confirmed cases from the same tour group or the same family as one, and excluded the cases that were related to the cruise ships because a large number of travelers being infected upon arrival made it difficult to trace the travel history of the first infected case. The travel case report data used in our analysis is provided in Appendix B.

For each travel origin, we also obtained the domestic case reports to model its growth curve as a comparison with the one estimated from the travel report. The city level data for Wuhan were obtained from [9]; and the country level data for United States, Italy, Iran and Egypt were obtained from COVID-19 Data Repository by the Center for Systems Science and Engineering (CSSE) at Johns Hopkins University [10].

2.2. Assumptions and key indicators of interest

In the initial phase of an emerging infectious disease outbreak, the infected cases and the recovered cases are both rare. So, the size of the susceptible population approximately equals to the whole population size, N . Let ρ_t be the prevalence rate (number of infected over total population size) t days after the epidemic first started. We assume that the prevalence rate increases

exponentially in this period,

$$\rho_t = \exp(\beta_0 + \beta_1 t), \quad (1)$$

where β_1 is the exponential growth rate. $N \cdot \exp(\beta_0)$ is the number of infected people when the epidemic first started. It came from each country's official announcement of their first confirmed case(s). In our study, this number is either 1 or 2. Note that the exact date of the first infection was hard to know, especially in the beginning of the outbreak, but some preliminary evidence might offer possible dates. We explored different possible start dates in the sensitivity analysis.

Another commonly used indicator, the doubling time, T_d , is given by $T_d = \log 2 / \beta_1$. The doubling time is the period that takes the number of infected individuals to double. Both the exponential growth rate (β_1) and the doubling time (T_d) measure the speed of the transmission which determines the scale of the epidemic.

Infection among medical professionals and death rate increase significantly when the health care system is overwhelmed. So, another important indicator we care about is the probability of the number of severe case patients exceeding the hospital capacity. Both the severe case patients and the hospital capacity are not evenly distributed within a country. Therefore, it would not make sense to compare the total number of severe case patients in a country to the national hospital capacity. Instead, we focused on one city level analysis (Wuhan) as an example.

2.3. Statistical modeling of the prevalence in the origin country

Our goal was to use the traveler case reports to infer the prevalence rate, or the exponential growth rate, in the origin country. For each origin, let n_{it} be the number of infected travelers who arrived at destination i at time t , and N_i be the size of average daily travelers of destination i in the study period. We assumed that the number of infected travelers followed a binomial distribution as below:

$$n_{it} | N_i, \rho_t, \alpha \sim \text{Binomial}(N_i, \rho_t \cdot \exp(\alpha)), \quad (2)$$

where ρ_t was the prevalence rate in the general population, and α captured the potential sampling bias in the travelers. If the group of travelers was a representative sample of the general population, the travelers would have the same rate of infection as the general population, so $\alpha = 0$. If for some

reason we believed that the travelers were more or less likely to get infected, we would expect a non-zero α .

Instead of using all of the reports up to the end date and providing one estimate of β_1 for each origin country, we provided daily update of β_1 to mimic the real-world decision making process. Specifically, for each origin, starting from the date with the first exported case report, t_1 , for all $t > t_1$, we ran the above model with all the data up to day t and provide a β_1 estimate. By doing so, we were able to see how the origin country’s β_1 estimate changed as the exported case reports accumulated, and when we could detect the outbreak with some consistency.

The destination countries with advanced public health infrastructures were more likely to detect the imported cases, and citizens from those countries might prefer returning to their countries for treatment when feeling sick. Therefore, it was possible that the groups of people who chose to travel to different destinations had different infection rates. We could address this heterogeneity by adding a destination specific random effect parameter b_i :

$$n_{it}|N_i, \rho_t, \alpha, b_i \sim \text{Binomial}(N_i, \rho_t \cdot \exp(\alpha + b_i)). \quad (3)$$

When fitting the real data, we tested the significance of this heterogeneity parameter b_i and found it not significant because of small sample sizes at the destination level. Therefore, we only reported results from the basic model as in (2).

We used Bayesian inference to estimate the parameters. Details about the choice of priors and hyper parameters are provided in Appendix A.2.

2.4. Imputing the missing arrival dates

In the initial period of the epidemic, there was not an airport-based traveler screening system. Therefore, a non-negligible proportion of arrival dates of the confirmed cases were missing in the early government and media reports. The accumulated missing proportions were 9.1% for Wuhan (China), 60.0% for United States, 89.5% for Italy, 88.9% for Iran and 66.7% for Egypt. To accurately estimate β_1 , it was necessary to impute those missing arrival dates by estimating the time interval between the arrival date and case confirmation date for each case. We modeled this time interval T_{ij} for destination i and case j by using a negative binomial distribution with a destination-specific mean μ_i and a dispersion parameter ϕ . In addition, some destination countries did not report any arrival dates of infected travelers. To estimate

the time intervals for those countries, we pooled μ_i towards a common mean. Specifically, the model was as follows:

$$\begin{aligned} T_{ij} | \mu_i, \phi &\sim \text{NegBinomial}(\mu_i, \phi) \\ \mu_i &\sim \text{Gamma}(\lambda, 1) \end{aligned}$$

Bayesian estimation was implemented and the choice of priors is provided in Appendix A.2. We used the observed pairs of arrival dates and confirmation dates to estimate the negative binomial parameters and generated posterior predictive distribution of the missing T_{ij} .

Finally, due to the delay of the diagnostic confirmation, we expected a proportion of travelers would not have been tested by the end of the study, and the undiagnostic rate would be higher in the later dates. For travelers arriving at destination i on day t , we down-scaled the average daily traveler size N_i by a factor of $q_{it} = P(T_{ij} \leq t_{\text{end}} - t)$, where t_{end} is the study end date and T_{ij} follows the negative binomial distribution. The final model we fitted was the following:

$$n_{it} | N_i, \rho_t, \alpha \sim \text{Binomial}(N_i \cdot q_{it}, \rho_t \cdot \exp(\alpha)), \quad (4)$$

Rather than imputing the missing arrival date with the posterior mean or median of T_{ij} , we fitted model (4) with each posterior sample of T_{ij} and the corresponding q_{it} . Therefore, the final uncertainty estimate of β_1 included the uncertainty of the missing arrival dates.

2.5. Comparison with the domestic data estimation

Our goal was to estimate the epidemic in the general population of those five origins by using their travelers data. As pointed out before, using only the travelers data might generate potential biases. We formally investigated the biases by comparing the estimates from the travelers data with the ones from the domestic case reports.

[11] carefully studied and reconstructed the full transmission dynamics in the early period of the COVID-19 epidemic in Wuhan by fitting a 7-compartment model. From their model output, we could derive the exponential growth rate before Jan 23, 2020 (assumed to be a constant) being 0.187 with 95% credible interval (0.178, 0.196). Unfortunately, similar results were not readily available for the other four travel origins due to limitations of the data and knowledge about their early stages. Instead, using the same data as in [9], we fitted an exponential growth model to the domestic daily

records of new infections. We found that for Wuhan (China), the directly fitted exponential growth rate was 0.175 with 95% confidence interval (0.160, 0.190). The large overlap between the two confidence intervals suggested that the exponential growth curve was a good approximation to transmission dynamic in the beginning of the disease outbreak. Therefore, for the other origins, we used the exponential growth rate fitted by this simple model using domestic records in [10] to serve as a comparison with the one estimated from the travelers data.

2.6. Estimating the probability of severe case exceeding hospital capacity

[12] estimated that 19.2% of infected individuals needed to be hospitalized. The number of hospital beds available to accept severe COVID-19 patients in Wuhan on January 21 was 800, according to [13]. We denote the number of severe case patients on day t by S_t , and $S_t = 0.192 \cdot N \cdot \rho_t$. For Wuhan, the probability that the number of severe cases exceed hospital capacity is then defined as

$$p_t = P(S_t > 800)$$

Using data up to day t , the posterior distribution of β_1 estimated from model (4) gave us the posterior distribution of S_t . From there, we updated p_t , the daily probability of hospital being overwhelmed.

2.7. Evaluating the traveler data impacts

In decision theory, we can evaluate the impact of a piece of information by comparing the risks with and without that information. The reduction in the risk is referred to as the value of information (VOI). In this study, we evaluated two types of impacts on estimating the exponential growth rate β_1 . They were 1. the traveler cases confirmed on day t , from the first date a travel case was confirmed to the end date of the study; and 2. knowing the actual arrival date of each case.

In Bayesian inference, when the goal is to provide a probabilistic estimate of a certain indicator, one proper risk is the integrated quadratic distance (IQD) [14], which measures the difference between two distributions. The IQD can be calculated as follows:

$$r(F, G) = E_{F,G}|\theta_F - \theta_G| - \frac{1}{2} \left[E_F|\theta_F - \theta'_F| + E_G|\theta_G - \theta'_G| \right], \quad (5)$$

where, in Bayesian decision theory, G is the estimated distribution and F is the true distribution of θ , θ_F is a random variable following the distribution F , θ_G is a random variable following the distribution G , and θ_F and θ'_F are two independent random variables following the distribution F . The true distribution is often unknown and thus replaced by the posterior distribution of θ given the full data. In that case, the VOI of any piece of information reduces to $r(F, G)$, where F is θ 's posterior distribution given the full data, and G is θ 's posterior distribution given the partial data by removing the piece of information we are interested in evaluating, such as missing arrival dates or one day's report [15].

For each day after the first case report, we would like to evaluate the influence of all available information on making the current day's decision. Specifically, to evaluate the impact of daily travel case reports on day t , we performed the following analysis.

1. Estimated the posterior distribution of β_1 given all the data up to day t , denoted as F_t .
2. For $i \leq t$, removed day i 's case report from the data, and estimated the posterior distribution of β_1 given the partial data, denoted by $G_{t(i)}^c$, where c stands for case reports. Calculated $r_{t(i)}^c$ using Equation (5), by setting $F = F_t$, and $G = G_{t(i)}^c$.

To evaluate the impact of knowing the arrival date, we performed the similar analysis. The only difference was setting $G = G_{t(i)}^a$ the posterior distribution of β_1 given the partial data that removed the arrival date of day i 's report, and imputed the missing arrival date following the procedure described in Section 2.4. The superscript a stands for arrival dates.

The procedure above allowed us to evaluate the information in three different aspects: 1. For each day's decision, rank the influence of all the previous days' case reports and the arrival dates; 2. For each day's decision, compare the influence of the number of cases v.s. knowing the arrival date for the same time point ($r_{t(i)}^c$ v.s. $r_{t(i)}^a$); and 3. As time moves forward, compare the influence of the same day's report ($r_{t(i)}^c$ v.s. $r_{t'(i)}^c$) and arrival date ($r_{t(i)}^a$ v.s. $r_{t'(i)}^a$).

Finally, when we remove a day's case report, we would like the effects to be purely due to the number of cases not observed, rather than a mix of not knowing the arrival date and not observing the cases. Therefore, we only performed this analysis on the Wuhan data since Wuhan only had one

missing arrival date in our study period while the rest of the origins all had over 50% of missing arrival dates.

2.8. Detecting future disease outbreaks

Finally, we would like to develop a useful tool for policy makers to determine the severity of a country's epidemic based on the number of exported cases. Statistically, we could form the question as a hypothesis testing problem. On each day, based on the cumulative number of exported cases up to that day, we could test whether the exponential growth rate is significantly above a certain threshold, for example 0.1.

$$H_0 : \beta_1 = 0.1 \quad v.s. \quad H_1 : \beta_1 > 0.1$$

We used a simulation based hypothesis testing procedure as follows:

1. Define the initial prevalence at a very low level such as one over the population size of the travel origin.
2. Calculate the time series of true prevalence rates following Equation (1) given the exponential growth rate at the null (H_0) value.
3. Let N be the daily average of outbound traveler sizes.
4. Generate a time series of daily number of infected travelers from the binomial distributions provided in Equation (2). Record the cumulative number of traveler cases up to each day since the first exported case.
5. Repeat Step 4 100,000 times. Summarize the empirical distributions of the cumulative number of traveler cases over the repetitions in two ways depending on whether the initial date of the local infection is known:
 - (a) If the initial date is known, we summarize the empirical distributions of the cumulative number of traveler cases stratified by the number of days since the initial local infection.
 - (b) If the initial date is unknown, we summarize the empirical distributions of the cumulative number of traveler cases stratified by the number of days since the first exported case. In this case, day 1 represents the date when the first exported case happens.

An extremely large number of traveler cases indicates a higher than expected growth rate.

6. Define a significance level and visualize the cumulative number of traveler cases that would be needed to reject H_0 for each day since the first exported case.

3. Results

The results section is organized in the following way. In Section 3.1 we present the results for the estimated time intervals between arrival date and case confirmation date by origin and destination. In Section 3.2, we illustrate how the estimated origin exponential growth rate and the doubling time changed as more case reports became available over time, and investigate the probability of severe COVID-19 cases exceeding the number of available beds in Wuhan, China. In Section 3.3, we conduct the sensitivity analysis to the initial number of cases. In Section 3.4, we discuss the impact of knowing the traveler cases and the travel dates on shaping the epidemic trend.

3.1. Time intervals between arrival and case confirmation

Figure 1 presents the distribution of time interval from arrival to diagnosis by origin: (a) Wuhan, China, (b) United States, (c) Egypt, (d) Iran and (e) Italy. Iran travelers had the shortest time interval with a median of 2.64 days shown by the pink dashed line and a 95% credible interval of (1.51, 4.20) days. The first exported case from Iran was confirmed on Feb 20, 2020. Iran announced the first two COVID-19 infection related deaths on Feb 19 [16], and reported 29 new cases by Feb 22. This might imply that other countries had set a higher detection priority to people traveling from Iran since Feb 19. For travelers from other places, the time intervals are summarized as follows. Wuhan, China has a median of 4.10 days and a 95% credible interval of (1.01,10.10) days; United States has a median of 6.01 days and a 95% credible interval of (1.69,13.90) days; Egypt has a median of 9.28 days and a 95% credible interval of (2.44, 21.10) days; Italy has a median of 9.64 days and a 95% credible interval of (3.86,18.79) days.

The time to diagnosis was further stratified by destinations using box plots in each sub-figure, and the destinations were arranged in an increasing order of the median time interval from top to bottom. We only presented results for destinations that had reported the arrival dates within the study

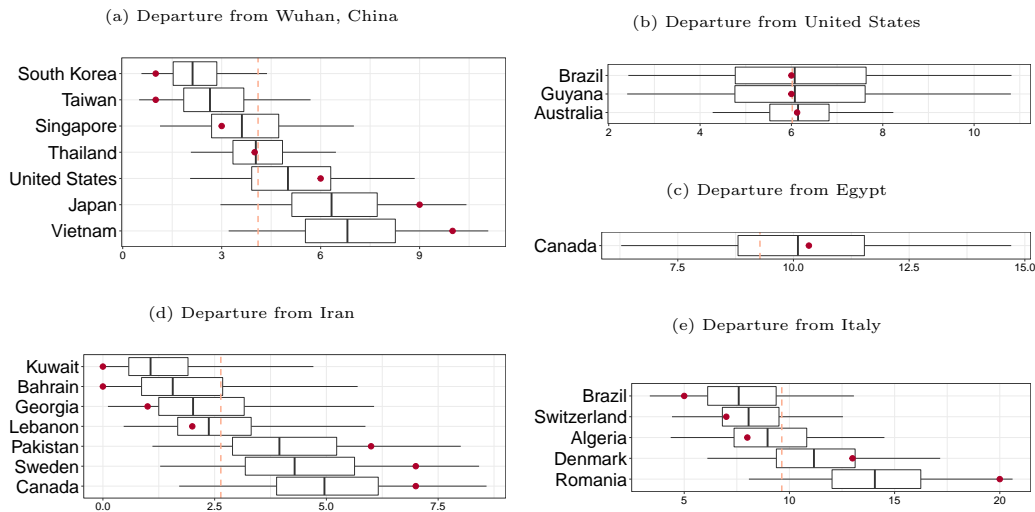
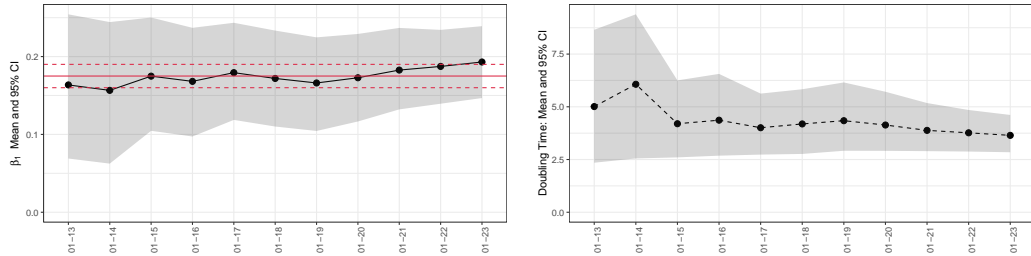


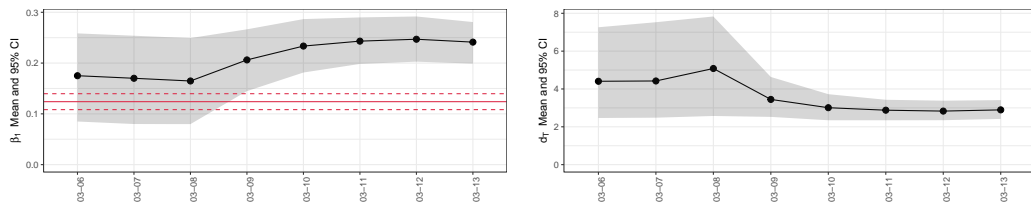
Figure 1: Posterior median, interquartile, and 95% credible interval of time to diagnosis by departure city/country and destinations. Each box represents the interquartile of the posterior of time to diagnosis by departure city/country, with the middle bar indicating the posterior median and the whisker showing the 95% credible interval. The red dots are observed time to diagnosis for the pairs of arrival dates and confirmed dates. The pink dashed line represents the overall median time to diagnosis across all destinations.

period. If a country had imported cases within the study period but did not release the arrival date of any case, then its median time interval would be the overall median across other destinations that had reported the arrival dates indicated by the pink dashed line. For China, Iran and Italy, most of the destinations are their neighboring countries. Before Jan 23, 2020, seven destinations detected COVID-19 cases among travelers from Wuhan. They were South Korea, Taiwan, Singapore, Thailand, United States, Japan, and Vietnam. By Aug 14, 2020, the numbers of reported COVID-19 related deaths were 7 in Taiwan, 21 in Vietnam, 27 in Singapore, 58 in Thailand, 305 in South Korea and 1,073 in Japan [10]. Those six places are among the strongest performers in the COVID-19 pandemic so far. The early detection of emerging infectious diseases among travelers did not only ring the alarm for the travel origin, but also allowed the destinations better prepare for the potential pandemic.

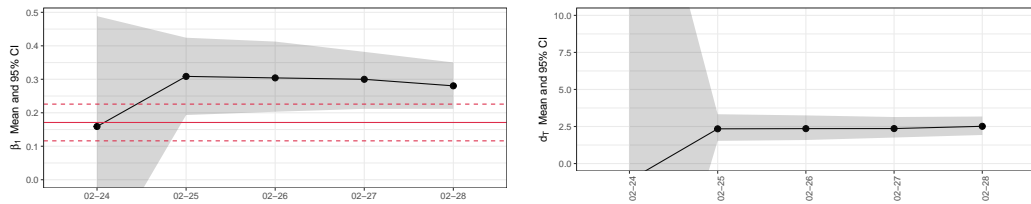
(a) $\hat{\beta}_1$ (left) and \hat{T}_d (right) in Wuhan, China between Jan 13 and Jan 23



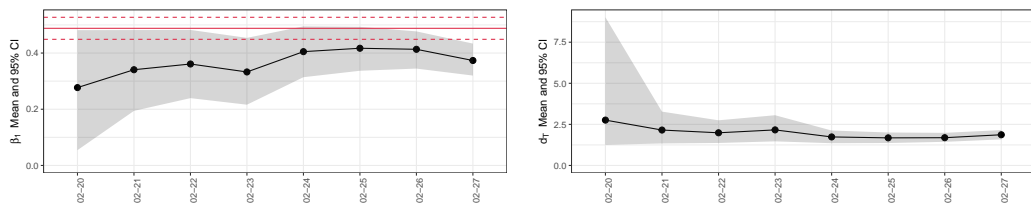
(b) $\hat{\beta}_1$ (left) and \hat{T}_d (right) in United States between Mar 6 and Mar 13



(c) $\hat{\beta}_1$ (left) and \hat{T}_d (right) in Italy between Feb 25 and Feb 28



(d) $\hat{\beta}_1$ (left) and \hat{T}_d (right) in Iran between Feb 20 and Feb 27



(e) $\hat{\beta}_1$ (left) and \hat{T}_d (right) in Egypt between Feb 28 and Mar 6

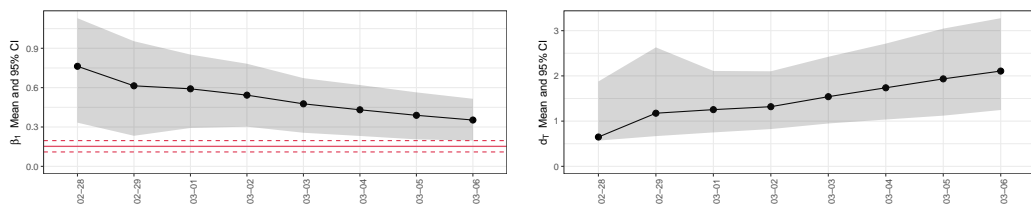


Figure 2: Posterior mean and 95% credible interval of exponential growth rate β_1 at early COVID-19 outbreak stage in (a) Wuhan, China, (b) United States, (c) Italy, (d) Iran, (e) Egypt. The black dots are the posterior mean and the grey bands are the 95% confidence credible intervals estimated from traveler data. The red horizontal lines indicate the mean (solid) and 95% confidence interval (dashed) estimated from domestic data.

3.2. Exponential growth rate, doubling time, and the probability of severe COVID-19 cases exceeding the hospital capacity

For each origin, we obtained estimates of the exponential growth rate, β_1 , and the doubling time, T_d , by fitting the model described in Section 2.3 to the traveler case reports up to different dates. Figure 2 visualizes how the mean estimates and 95% uncertainty bounds of β_1 and T_d changed as more confirmed cases became available over time.

The sequential updates of $\hat{\beta}_1$ and \hat{T}_d became more stable over time. For all travel origins, within three days after the initial exported case report, the estimated lower bound of the exponential growth rate was above 0.1, which corresponded to the doubling time being significantly less than one week. Table 2 summarizes the dates on which the estimated exponential growth rate, β_1 , was significantly greater than 0.1. We found less than ten exported case reports would be needed and the detection dates were within three days after the first exported case report for all countries.

Table 2: The dates on which the estimated exponential growth rate, β_1 , was significantly greater than 0.1. For each date, we also provide the number of days after the first exported case confirmation and the cumulative number of exported case reports.

	detection date	number of days	number of cases
Wuhan	Jan 15	2 days	2 cases
U.S.	Mar 9	3 days	3 cases
Italy	Feb 25	1 day	9 cases
Iran	Feb 21	1 day	2 cases
Egypt	Feb 28	0 day	1 case

The estimated exponential growth rate in Wuhan, Iran, Italy and United States showed an overall increasing trend at the beginning of the outbreak after the confirmation of the first exported case. The decreasing trend of $\hat{\beta}_1$ in Egypt was because we assumed the epidemic in Egypt started on Feb 14, 2020 with only one infected individual on that date. A high level of growth rate would be needed to observe many traveler cases between March 1, 2020 and March 6, 2020. Since the travel date of the first exported case from Italy (confirmed on Feb 24, 2020) was unknown, $\hat{\beta}_1$ and \hat{d}_T had a larger uncertainty when only observing the first exported case.

To compare the estimates from travelers data with the ones from domestic data, we fitted exponential growth curves to the domestic daily records using

[9] for Wuhan (China) and the COVID-19 Data Repository [10] for United States, Italy, Iran and Egypt. To maximize the sample size, we chose the end date of the domestic data to be 5 days (the mean incubation period) after the country announced national emergency or implemented lock-down order. The mean estimates and confidence intervals of the growth rates were 0.175 (0.160, 0.190) for Wuhan (China), 0.124 (0.108, 0.140) for United States, 0.171 (0.116, 0.226) for Italy, 0.488 (0.449, 0.527) for Iran, 0.153 (0.110, 0.196) for Egypt. We indicated these estimates and intervals with horizontal red lines in Figure 2. The domestic data mean estimates for United States, Italy and Egypt were significantly lower than the traveler data based estimates. Some possible reasons for the discrepancy include: (a) their initial numbers of cases were larger (see sensitivity analysis in Section 3.3); (b) the number of infected increased faster than the testing capacity in the early period; (c) the number of travelers had declined within the study period; and (d) the travelers did not represent the general population thus could bear a higher or lower infection rate. (a) and (b) could lead to underestimated growth rate using domestic data. (c) could lead to overestimated growth rate using traveler data. (d) could lead to either direction of biases.

In Figure 3, we plotted the probability of severe COVID-19 cases exceeding the number of available beds in Wuhan. With the first exported case confirmation on Jan 13, the probability was at a relatively low level around 26%. It jumped to 54% when the third exported case was confirmed on Jan 17, and kept increasing as new case reports became available over time. The probability exceeded 90% on Jan 23, indicating that hospitals would soon be overwhelmed with COVID-19 patients.

3.3. Sensitivity analysis to the initial number of cases

In the previous analysis, we assumed the epidemic start date for each origin as the date when they announced their first case(s), denoted as t_0 . In this section, we investigated how the estimate of the exponential growth rate, $\hat{\beta}_1$, would have changed if the epidemic had started earlier. An earlier starting date is equivalent to there were more cases at t_0 than 1 or 2. We reran the analysis with the number of cases at t_0 being 10, 100, and 1000 respectively.

Figure 4 presents the estimated exponential growth rates using traveler data and different initial number of cases, as well as the exponential growth rates estimated from domestic data (red horizontal lines). The black lines indicated the original model fits assuming that the number of initial cases was

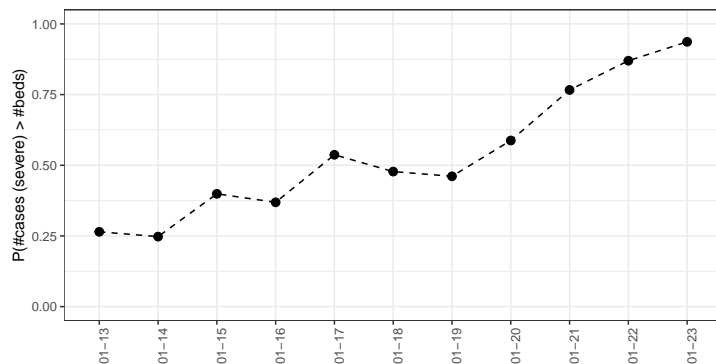


Figure 3: Posterior probability of the number of severe cases exceeds the number of available hospital beds in Wuhan China during Jan 13, 2020 - Jan 23, 2020.

either 1 or 2 at t_0 . A larger number of initial cases corresponded to a lower estimate of the exponential growth rate. For Wuhan and Italy (panels (a) and (c) in Figure 4), the current assumed initial case number (epidemic start date) seemed to be reasonable. For Iran (panel (d)), the first government announcement in Iran regarding to COVID-19 was two deaths on Feb 19, 2020 [16]. We assumed that the start date was 20 days before, based on that the first COVID-19 related death in Wuhan was on Jan 9, 2020 with symptom onset on Dec 20, 2019. This appeared to be a reasonable assumption given the traveler data estimates (black) crossing the domestic data estimated interval (red) in the end. For United States, Italy and Egypt (panels (b), (c) and (e)), their 95% credible intervals at the end date of study period were above the domestic data estimates which better matched with “100 cases” scenario or “1000 cases” scenario.

There were two reasons that we might set the initial number of cases at a higher level: one was the under-reporting of initial cases; and the other was the epidemic being limited to a sub-national area where the ratio between the traveler size and the local population size was much higher than the national average. Note that we had used the national population as the reference to calculate the initial COVID-19 prevalence rates in United States, Italy, Iran and Egypt. If the outbreak was limited within a sub-national area, one should adjust both the reference population size and the traveler size from the national level to the sub-national level. This would not affect the estimate of the growth rate if the ratio between the traveler size and

reference population size at the sub-national level is equal to that ratio at the national level. However, for areas such as tourism sites, the ratio between traveler size and the reference population size could be much higher than the national average. For instance, [17] commented that “Egypt is an agricultural country. Most tourism destinations are in special locations far away from residential places and have low population densities.” If the Egypt outbreak was indeed only at the tourism destinations where the reference population size was small but the international traveler volume was large, then $\hat{\beta}_1$ for the tourism destinations in Egypt should be similar to “100 cases” or “1000 cases” scenario in Figure 4 (e), which did not have the surprisingly high estimates in the first couple of days, and better matched with the estimates from the domestic daily records. Unfortunately, most traveler case reports only provided the countries being visited but not the sub-national areas.

We also noticed that the prevalence ρ_t in the origin was less sensitive to the assumption of the start date. Therefore, the total number of cases and severe cases were similar in different scenarios. As seen in Figure 4 (f), the probabilities of the number of severe cases exceeding the number of available hospital beds in Wuhan China were similar.

Finally, we found that the differences of $\hat{\beta}_1$ s among different scenarios of initial cases became smaller as more traveller case reports became available over time. The effect of initial number of cases will be addressed quantitatively in Section 3.4.

3.4. Impact of daily traveler case reports and travel dates

As described in the Methods section, we conducted a series of analysis on the Wuhan outbound traveler case report data to evaluate the influence of different information on each day’s estimate. Every time a new case report was observed, we computed the value of information of all of the previous case reports on making the current day’s decision (estimation). The case reports among Wuhan travelers were available on Jan 13 (one case), Jan 15 (one case), Jan 17 (one case), Jan 20 (one case), Jan 21 (two cases), Jan 22 (two cases), and Jan 23 (three cases). Figure 5 presents the value of information (VOI) analysis results. Figure 5 was organized by decision (estimation) date. In each sub-figure, we calculated the VOI of all of the case reports up to this date on estimating the current β_1 , and displayed them using the blue line. We also calculated the VOI of knowing each arrival date on estimating the current β_1 , and displayed them using the red line. We had the following findings:

1. For the days with the same number of cases, we observed that the more recently confirmed cases had higher VOI than the earlier cases, except that the case on 01-13 had a higher VOI than the case on 01-15. This was because for all the other cases, the earlier the arrival dates, the earlier the confirmed date (for the date with multiple confirmations we looked at the average arrival date). However, the arrival date of the 01-15 case was earlier than the 01-13 case. Therefore we concluded that the more recent arrival cases had higher VOIs.
2. From sub-figures (d), (e) and (f), we observed that the days with a larger number of case confirmations had a larger VOI.
3. Each case report's VOI decreased over time. This was because first each case became less recent as we moved along the decision date, and second as more case reports became available, the expected loss of removing one case report got smaller.
4. In terms of knowing the arrival dates, in general, it was also true that the more recent arrival dates had higher VOIs. In addition, the more cases in each report, the larger its VOI was. Note that one of the two cases on 01-22 had missing arrival date, and thus the VOI of 01-22 arrival dates measured the effect of removing one arrival date.
5. Comparing the VOI of the case reports and the VOI of the arrival dates, we found that in general the case reports had higher VOIs than the arrival dates and the gap was larger for more recent dates. Note that the arrival date of the 01-15 case was 01-06 (the slowest time to diagnosis) and the arrival date of the 01-20 case report was 01-19 (the fastest time to diagnosis). Their arrival date VOIs were very close to (and sometimes exceeded) the case report VOIs. It suggested the case reports would be less useful without arrival dates, especially when the time to diagnosis was much longer or shorter than the average, which made the imputation inaccurate.

3.5. Number of cases needed to detect the disease outbreak

To demonstrate how many exported cases needed to detect a disease outbreak with certain statistical significance, we conducted the hypothesis test of whether the exponential growth rate exceeded 0.1. We used the initial prevalence, 0.01%, corresponding to one initial infection in a place with one million people, and set daily average of outbound traveler size at $N = 1,000$.

Figure 6 illustrates the minimum required cumulative number of traveler cases for each day to detect $\beta_1 > 0.1$, in the case of known (top) and unknown (bottom) initial local infection date. The significance levels were set to be 0.05, 0.01 and 0.001. First of all, more traveler cases were needed to draw the conclusion at a higher significance level. The number of cases needed increased as the epidemic went into a later period. In an extreme case, if on the first day of the epidemic there was already an exported case, we would be highly confident that the local infection rate was very high. When making decisions to detect a future disease outbreak on a certain day, if we have relatively accurate information about how long it has been since the first local infection, we can use the top figure to compare the total number of exported cases up to this day. At a pre-specified significance level, say 5%, if the total number has exceeded the number of the corresponding date in the figure, we would be able to tell that with 95% confidence the local epidemic has an exponential growth rate bigger than 0.1. If we do not know the initial infection date, we would count how many days it has been since the first exported case, and compare with the bottom figure.

A Shiny App for implementing the above hypothesis testing was provided in Appendix C, where users could specify the initial prevalence, the null hypothesis, the daily average of outbound traveler sizes, the number of simulations, and the significance level. With this tool, policy makers could adjust the parameters to fit their own country's situation, and quickly determine how severe their country's epidemic is based on the exported cases.

4. Discussion

We used the COVID-19 epidemic as an example to illustrate how the traveler case reports could be used to detect a disease outbreak at early stage. We found that the dates that our estimated indicators exceeded certain threshold (exponential growth rate were significantly above 0.1 (doubling time < 7 days), and probability of COVID-19 patients exceeding hospital capacity $> 90\%$) were all within the period that critical policies (city lockdowns and announcing national emergencies) were made based on domestic data. In general, using the traveler data was effective in detecting a disease outbreak in the travel origin.

From the data impact study, we found that knowing the actual arrival dates improved the estimates. In addition, more detailed travel history at sub-national level helped countries identify whether the outbreak was within

a region or at the national level. For instance, without such information for patients with travel history to Egypt, we could not tell whether the initial epidemic was limited to tourism sites. Given the spreading speed of an emerging infection, it would be desirable to have early warning at sub-national levels. The proposed method can also detect the emerging disease outbreak at sub-national level if the sub-national surveillance system traces and reports the travel history of patients who have visited other sub-national areas. Implementation of such analysis requires travel size estimates across sub-national units in addition to the traveler case reports.

When comparing the estimates from the traveler data to the ones from domestic data, we found that the using only the traveler data had several limitations. One would need relatively accurate information about when the epidemic first started in the travel origins. A large estimate of exponential growth rate from the travel data could imply either a fast growth rate or a severe under-reporting of initial cases. More fundamentally, how well one can estimate the domestic epidemic using the traveler data depends on how representative the traveler samples are. As an extreme example, if the travelers were all young adults with good health, using the traveler data would've underestimated the epidemic in the general population. In our model, we introduced a non-zero intercept β_0 in the exponential growth curve, trying to correct the sampling bias. However, without further information, we could only use a non-informative prior on β_0 . Studies that could potentially improve this sampling bias correction include, but are not limited to, better understanding the travelers' demographics, such as age, gender, sub-national region of residence, etc.

Finally, we provided an easy-to-use tool for policy makers to determine the growth rate of local epidemic based on exported cases. A user-friendly Shiny App was developed to accommodate flexible scenarios that fit different countries' situations.

Rapid detection of early disease outbreak is crucial for government intervention and raising public awareness. The traveler case reports data seems to be a good addition to the domestic surveillance data by utilizing the diagnosis resources from all countries. We advocate that countries should work in a collaborative way, by sharing the traveler patients information about the travel dates and more detailed travel history at sub-national level, in a timely manner. Working together, we would strengthen the global infectious disease surveillance system, which is especially important in detecting disease outbreaks in countries where public health infrastructure is rudimentary or

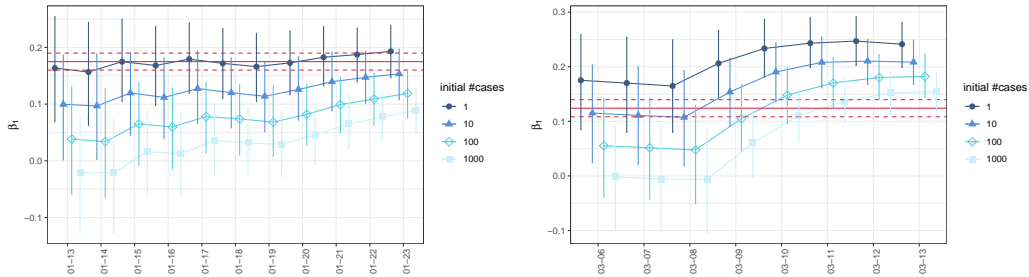
nonexistent.

References

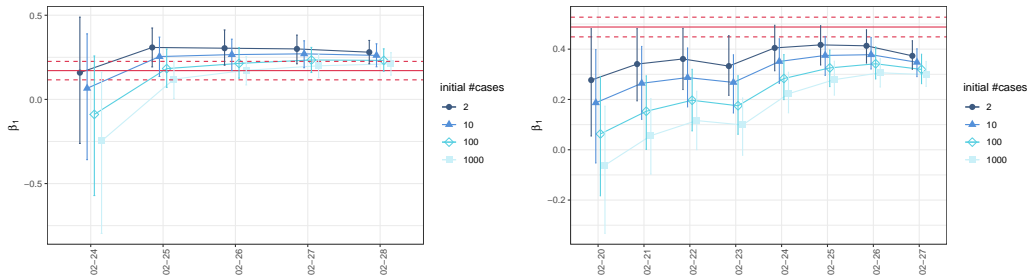
- [1] World Health Organization (WHO) Emergency Committee, Statement on the second meeting of the International Health Regulations (2005) emergency committee regarding the outbreak of novel coronavirus (2019-ncov) (2020).
- [2] D. L. Heymann, G. R. Rodier, et al., Hot spots in a wired world: WHO surveillance of emerging and re-emerging infectious diseases, *The Lancet Infectious Diseases* 1 (2001) 345–353.
- [3] S. S. Morse, Global infectious disease surveillance and health intelligence, *Health Affairs* 26 (2007) 1069–1077.
- [4] M. E. Wilson, Travel and the emergence of infectious diseases., *Emerging infectious diseases* 1 (1995) 39.
- [5] J. T. Wu, K. Leung, G. M. Leung, Nowcasting and forecasting the potential domestic and international spread of the 2019-ncov outbreak originating in Wuhan, China: a modelling study, *The Lancet* 395 (2020) 689–697.
- [6] N. Imai, I. Dorigatti, A. Cori, C. Donnelly, S. Riley, N. M. Ferguson, Report 2: Estimating the potential total number of novel coronavirus cases in Wuhan City, China, Imperial College London (2020).
- [7] M. Chinazzi, J. T. Davis, C. Gioannini, M. Litvinova, L. Rossi, X. Xiong, M. E. Halloran, A. Vespignani, Preliminary assessment of the international spreading risk associated with the 2019 novel coronavirus (2019-ncov) outbreak in Wuhan city, *Lab. Model. Biol. Soc.–Techn. Syst* (2020).
- [8] B. Xu, B. Gutierrez, S. Mearu, K. Sewalk, L. Goodwin, A. Loskill, E. L. Cohn, Y. Hswen, S. C. Hill, M. M. Cobo, et al., Epidemiological data from the covid-19 outbreak, real-time case information, *Scientific Data* 7 (2020) 1–6.

- [9] A. Pan, L. Liu, C. Wang, H. Guo, X. Hao, Q. Wang, J. Huang, N. He, H. Yu, X. Lin, et al., Association of public health interventions with the epidemiology of the covid-19 outbreak in wuhan, china, *The Journal of the American Medical Association* 323 (2020) 1915–1923.
- [10] The Center for Systems Science and Engineering (CSSE) at Johns Hopkins University, (COVID-19) data repository, <https://github.com/CSSEGISandData/COVID-19>, 2020.
- [11] X. Hao, S. Cheng, D. Wu, T. Wu, X. Lin, C. Wang, Reconstruction of the full transmission dynamics of covid-19 in wuhan, *Nature* (2020) 1–7.
- [12] W. Liang, W. Guan, C. Li, Y. Li, H. Liang, Y. Zhao, X. Liu, L. Sang, R. Chen, C. Tang, et al., Clinical characteristics and outcomes of hospitalised patients with COVID-19 treated in Hubei (epicenter) and outside Hubei (non-epicenter): A nationwide analysis of China, *European Respiratory Journal* (2020).
- [13] Xinhua Net, Wuhan: Three designated hospitals treat patients with new coronavirus infection and pneumonia confirmed for free treatment, http://www.xinhuanet.com/2020-01/21/c_1125491413.htm, 2020.
- [14] T. L. Thorarinsdottir, T. Gneiting, N. Gissibl, Using proper divergence functions to evaluate climate models, *SIAM/ASA Journal on Uncertainty Quantification* 1 (2013) 522–534.
- [15] J. Parsons, L. Bao, The value of information in retrospect, *arXiv preprint arXiv:1806.01458* (2018).
- [16] World Health Organization, et al., Coronavirus disease (COVID-2019) situation reports, 2020.
- [17] A. Negida, Comments on the estimation of the covid-19 burden in Egypt through exported case detection, *The Lancet Infectious Diseases* (2020).

(a) $\hat{\beta}_1$ in Wuhan between Jan 13 and Jan 23 (b) $\hat{\beta}_1$ in United States between Mar 6 and Mar 13



(c) $\hat{\beta}_1$ (left) in Italy between Feb 24 and Feb 28 (d) $\hat{\beta}_1$ in Iran between Feb 20 and Feb 27



(e) $\hat{\beta}_1$ in Egypt between Feb 28 and Mar 6 (f) Probability of the number of severe case patients exceeds the hospital capacity in Wuhan, China

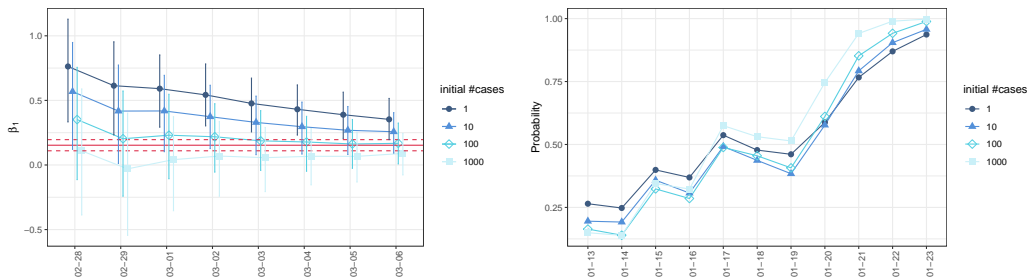


Figure 4: The estimated exponential growth rate, $\hat{\beta}_1$, under different initial number of cases in (a) Wuhan, China, (b) United States, (c) Italy, (d) Iran, (e) Egypt. The red horizontal lines indicate the mean (solid) and 95% credible interval (dashed) estimated from domestic data. (g) the estimated probability of the number of severe case patients exceeds the hospital capacity under different initial number of cases in Wuhan, China. The dots are the posterior mean and error bars are the 95% confidence credible intervals. Different color represents different initial number of cases.

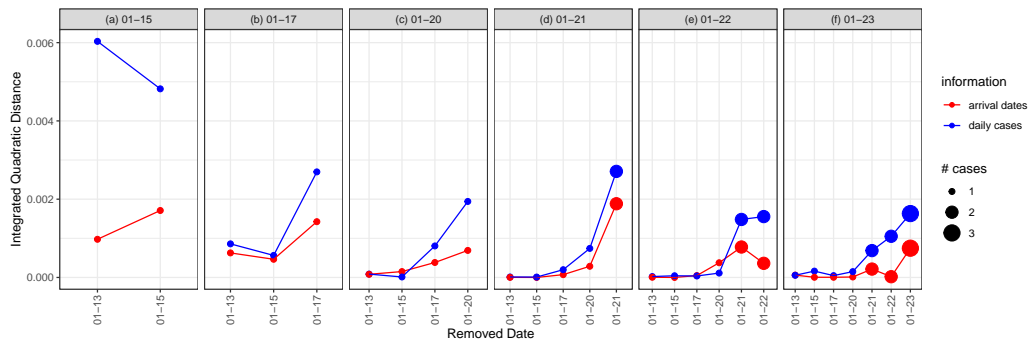
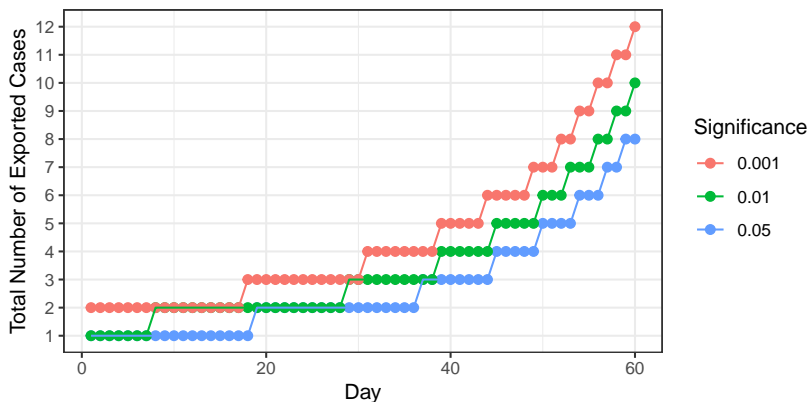


Figure 5: The value of information (VOI) of daily case and arrival date reports during Jan 13 - Jan 23. The blue lines are the VOIs of daily case reports. The red lines are the VOIs of daily arrival date reports. Each sub-figure corresponds to estimating β_1 on a different date t , shown as the sub-title.

(a) Total number of exported cases stratified by the number of days since the initial local infection



(b) Total number of exported cases stratified by the number of days since the first exported traveler case

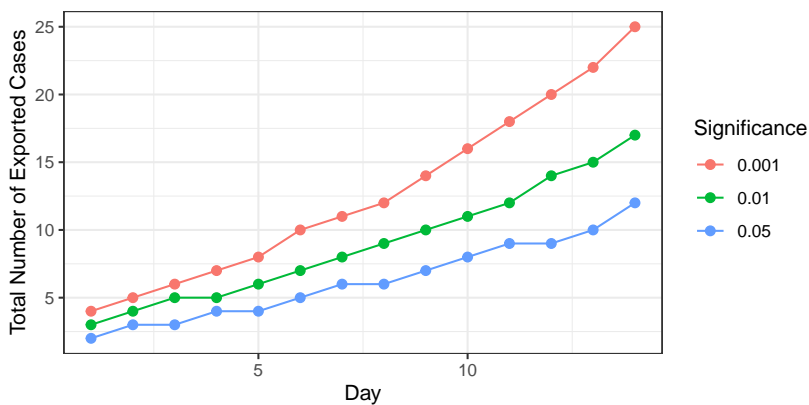


Figure 6: Hypothesis test of whether the exponential growth rate exceeds 0.1. The require cumulative total of traveler cases to reject the null hypothesis. The tests were conducted under three different significance levels: 0.05 (blue), 0.01 (green), and 0.001 (red). The x-axis indicates (a) the number of days since the initial local infection, (b) the number of days since the first exported case. The y-axis indicates the cumulative total of exported cases at the day indicated by x-axis.